Journal of the Korean Physical Society, Vol. 28, No. 6, December 1995, pp. 734~739

Growth Rate Calculation and One-dimensional Simulation of an Electromagnetically Pumped FEL

Tae Hun CHUNG
Department of Physics, Dong-A University, Pusan 604-714

Jae Koo LEE
Department of Physics, Pohang University of Science and Technology, Pohang 790-784

(Received 1 August 1995)

The dispersion relation of the scattered electromagnetic wave for an electromagnetically pumped free-electron laser is numerically solved. In addition, one-dimensional coupled Maxwell-Lorentz equations are derived, and a particle simulation of the performance of the FEL amplifier in the long-pulse limit is performed for various pump conditions. The effect of the axial guide field, the beam energy and energy spread, and the pump strength on the system are investigated. Finally, the requirements on the electron beam quality and the parameter region of practical interest are discussed.

I. INTRODUCTION

Since the successful experiment at Stanford [1], free-electron laser(FEL) has become a promising device to generate tunable coherent radiation over at wide range of wavelengths. A considerable amount of effort has been directed toward a scheme which utilizes the stimulated scattering by a static, transverse magnetic field. Although, in principle, one can cover the whole spectrum of electromagnetic radiation, one needs very high electron energy to obtain a frequency of infrared or higher since conventional magnetic wigglers have period on the order of a centimeter.

An alternative approach to shorten the FEL wavelength is to use an electromagnetic (EM) wave as the wiggler field. Recent technological advances have made possible EM wave sources having high intensities, modest energies, and short pulses [2]. Radiation sources, such as high power klystron, gyrotrons, or CO_2 lasers could be appropriate candidates for providing the pump EM wave because of the requirement of a high degree of phase stability [3]. High-quality electron beams of relatively low energy (1–3 MeV) from electrostatic accelerators, photocathode injectors, and microwave guns appear to be promising beam sources for an EM wiggler FEL.

Microwave undulators have been used for the generation of synchrotron radiation in the visible region of the spectrum using high voltage electron beams [4]. The EM wiggler fields may be stored in a high-Q cavity or they may be travelling in a waveguide or free space [5,6]. In addition, gyrotron-powered standing-wave EM wiggler experiments have been performed [7], and a compact laser synchrotron source based on the Thomson backscattering of intense laser radiation from a counterstreaming electron beam has been proposed [8]. A coherent beam of X-ray photons will be produced by Compton backscattering of visible light from a conventional FEL by the same bunched electron beam in the stable resonator [9].

The resonance condition $\lambda = \lambda_0(1 + K^2)/4\gamma_0^2$ (where λ is the wavelength of the emitted radiation, λ_0 the wavelength of the pump EM wave, and γ_0 the relativistic factor) is assumed. Here, the undulator parameter $K(= e\lambda_0 E_0/2\pi mc^2)$ depends on the pump-laser intensity $S(= c\epsilon_0 E_0^2)$. However, the laser intensity cannot be assumed to be constant throughout the focal region and this fact might prevent the effective resonance condition and, consequently, cause a strong reduction of the gain [10]. Although K^2 will normally be much less than unity, its effect on the resonance condition cannot, in general, be neglected because a small change in K^2 may become significant when it accumulates over a large number of undulator periods [11].

In this paper, we consider an electromagnetic travelling-wave free-electron laser. A pump wave is applied in the opposite direction to that of a free stream of electrons (counter propagating scheme). An axial guide magnetic field may be superimposed to steer the electron propagation along the axis. The presence of the axial guide field is a necessity in intense ($I > 1$ kA) relatively low energy ($\gamma_0 < 10$) electron-beam experiments. In this case, a circularly polarized pump wave is used, and the scattered EM wave has two cyclotron modes of polariza-

tion, that is, a left-handed circularly polarized (LHCP) and a right-handed circularly polarized (RHCP) mode [12]. Enhanced growth rates are reported when the frequency of the pump in the beam frame approaches the electron cyclotron frequency.

The growth rate can be calculated solving the linear dispersion relation. We calculate the growth rate of the scattered EM wave for various cases (for instance, with varying electron energy and with varying strength of the axial guide magnetic field) and determine the optimal conditions which yield the largest value of the growth rate.

We formulate the 1-D coupled Maxwell-Lorentz equation [13] which can be used for a one-dimensional simulation of the particle transport. Since the process of the generation and amplification of the emitted wave is very sensitive to the phase between the electron and the pump wave, particle simulation can give a proper estimate of the FEL performance. Using the code, we perform a series of simulations and compare the simulation results with the growth rate obtained from the linear dispersion relation. Another problem lying in this scheme (using a mildly relativistic electron beam) is the quality of the electron beam; this is especially so in a high-frequency region. A rough estimate for the required emittance is given by the inequality $\epsilon < \lambda$. Another aspect of the electron beam quality can be described in terms of the axial energy spread, or the axial momentum spread. We correlate these with the scattering parameter $k\lambda_D$ (where k is the wavenumber of the scattered wave and λ_D is the Debye length in the electron beam).

The organization of this paper is as follows: Section II provides a brief summary of the dispersion relation for the scattered radiation. Section III gives the steady-state Maxwell-Lorentz equations which serve as a simulation model for the electromagnetically pumped FEL. Section IV describes the results of the calculation and presents a discussion. Section V summarizes conclusions.

II. DISPERSION RELATION

The dispersion relation in the case of a circularly polarized travelling-wave wiggler field is written as [12]

$$D_L^R D_{ES} = \frac{F\omega_p^2 V_0^2 k^2}{2\gamma_0^3} \tag{1}$$

where

$$D_L^R = \left(\omega - kv_0 \mp \frac{\Omega_{ce}}{\gamma_0}\right)(\omega^2 - k^2c^2 - F\omega_p^2) \mp \frac{F\Omega_{ce}}{\gamma_0}\omega_p^2,$$

$$D_{ES} = (\omega \mp \omega_0 - kv_0)^2 - \frac{\omega_p^2}{\gamma_0^2}(1 + 3k^2\lambda_D^2\gamma_0^2).$$

Here Ω_{ce} is the gyrofrequency of the electron, ω_p is the relativistic plasma frequency, $\gamma_0 = 1/\sqrt{1-\beta_0^2}$ ($\beta_0 = v_0/c$, v_0 is the propagation velocity of the relativistic electrons), and (ω_0, k_0) and (ω, k) are the frequency and the wavenumber of the pump wave and the scattered wave, $\overline{\omega_0} = \omega_0 + k_0 v_0$, and R and L denote the RHCP and LHCP, respectively. F is the beam filling factor, and V_0 is the quivering velocity which is related to the pump intensity S by

$$V_0 = c\beta_\perp = \frac{e\lambda_0}{\gamma_0 \pi mc}\left[\frac{S}{4\epsilon_0 c}\right]^{\frac{1}{2}}. \tag{2}$$

Note that $D_L^R = 0$ is the dispersion relation for the uncoupled circularly polarized EM mode, and $D_{ES} = 0$ is that for the uncoupled electron-beam mode. The pump frequency ω_0 is chosen as [12]

$$\omega_0 = \frac{1}{2}\left[\frac{\Omega_{ce}}{\gamma_0} + \sqrt{\left(\frac{\Omega_{ce}}{\gamma_0}\right)^2 + 4\omega_p^2}\right], \tag{3}$$

which is calculated as the cutoff frequency (ω_{co}) from the dispersion relation for the pump EM wave.

One of the motivations of this study is to investigate the effect of the detuning energy spread on the growth rate (or the power gain) of the scattered EM wave. The detuning spread is caused by axial energy spread, finite beam emittance, space charge, and transverse field inhomogeneity. This can be pursued in several ways. In this study, first we solve the dispersion relation which contains the thermal spread of the electron beam and obtain the complex zeroes by the Müller method [14]. In the particle simulation, we can handle the detuning of energy directly.

The electron beam emitted from the cathode of the accelerators has an intrinsic energy spread. Especially for a mildly relativistic electron beam, the beam has a considerable thermal spread. Before entering the undulator, the beam has an intrinsic transverse component of motion, v_x/v_z , due to the finite cathode temperature, non-ideal electron optics, etc. The divergence is expressed in terms of an emittance ϵ/x where x is the transverse dimension. The axial energy spread due to the emittance is then [15]

$$\left(\frac{\Delta\gamma_z}{\gamma_0}\right)_\epsilon = \frac{1}{2}\left(\frac{\epsilon_n}{r_b}\right)^2 \frac{1}{1+K^2} \tag{4}$$

where ϵ_n is the normalized emittance, r_b is the beam radius, and K is the undulator parameter. Besides this effect, the axial energy spread arises from the self-potential of the beam resulting from space-charge and from the contribution due to wiggler gradients [15,16]. These are written as

$$\left(\frac{\Delta\gamma_z}{\gamma_0}\right)_{sc} = \frac{\nu}{\gamma_0}, \tag{5}$$

$$\left(\frac{\Delta\gamma_z}{\gamma_0}\right)_\omega = \left(\frac{r_b\omega_{ce}}{2c}\right)^2 \tag{6}$$

where ν is the Budker parameter of the beam and ω_{ce} is the gyrofrequency of the electron in the wiggler magnetic field. Equations (4)-(6) contribute to the global axial energy spread. A poor quality beam causes the gain line shape to be inhomogeniously broadened. At high energy, the principal contribution arises from the emittance of the beam. However, for low (or moderate) energy, high current electron beam, the diode emittance is negligible compared with that arising from other two origins. In principle, the beam emittance and the space charge forces should be addressed by a full three-dimensional theory to take into account all the possible detrimental effects on FEL gain, modeling these effects with an equivalent axial energy spread (or scattering parameter) allows only the longitudinal velocity modulation to be considered.

III. PARTICLE SIMULATION MODEL

We consider a steady state condition in which the radiation amplitude increases with distance, but not with time, through the interaction region. Also, a continuous electron beam is employed to avoid the complexity associated with lethargy. The motion of an electron in the combined pump and scattered EM wave is derived as

$$\frac{d\gamma}{dz} = -\frac{ka_s a_p}{\gamma}\sin\psi - a_z, \tag{7}$$

$$\frac{d\psi}{dz} = 2k_0 + \frac{(k_0 - k)}{2\gamma^2}[1+\alpha^2] + \frac{d\phi_s}{dz} + \frac{d\phi_p}{dz} \tag{8}$$

where

$$\psi = (k+k_0)z - (\omega-\omega_0)t + \phi_s + \phi_p,$$
$$\alpha^2 = a_s^2 + a_p^2 - 2a_p a_s \cos\psi.$$

Here, γ is the relativistic factor of the electron beam, k_0 and k are the wavenumbers of the pump and the scattered EM waves respectively, ϕ_p is the phase of the pump EM wave, and ϕ_s is the phase of the scattered EM wave. a_s and a_p are the normalized amplitudes of the scattered EM wave and the pump EM wave, respectively, and a_z is the normalized longitudinal electric field [17]. Assuming a single frequency, the scattered wave and the pump wave evolve according to

$$\frac{da_s}{dz} = a_p\kappa\left\langle\frac{\sin\psi}{\gamma}\right\rangle, \tag{9}$$

$$\frac{da_p}{dz} = -a_s\kappa\frac{k}{k_0}\left\langle\frac{\sin\psi}{\gamma}\right\rangle, \tag{10}$$

$$\frac{d\phi_s}{dz} = \frac{a_p}{a_s}\kappa\left\langle\frac{\cos\psi}{\gamma}\right\rangle - \kappa\left\langle\frac{1}{\gamma}\right\rangle, \tag{11}$$

$$\frac{d\phi_p}{dz} = -\frac{a_s}{a_p}\kappa\frac{k}{k_0}\left\langle\frac{\cos\psi}{\gamma}\right\rangle + \kappa\frac{k}{k_0}\left\langle\frac{1}{\gamma}\right\rangle \tag{12}$$

where $\kappa = \omega_p^2/2kc^2$ and $\langle..\rangle$ is the ensemble average.

Although the derivation of Eqs. (7)-(12) is started in Ref. 13, the present form is more useful and suitable for the particle simulation. Similar formulations can be found in Refs. 18, 19, and 20. Those formulations can be used for calculation of the pump depletion and the signal diffraction [20]. When an axial guide magnetic field is employed, the radiation amplitude a_p should be modified to $\overline{a_p}$ as

$$\overline{a_p} = \frac{a_p}{1-r}, \qquad r = \frac{\Omega_{ce}}{\gamma\omega_0}. \tag{13}$$

From Eqs. (9) and (10), we can note

$$k\frac{d}{dz}|a_s|^2 = -k_0\frac{d}{dz}|a_p|^2. \tag{14}$$

Since the photon number density scales as $N \sim k|a|^2$, the conservation of photon is recovered.

It is possible to evaluate the depletion of the pump wave for a steady-state amplifier with an interaction length L. Assuming that the radiation field grows exponentially (with growth rate Γ), the radiation and the pump fields are written as

$$|a_s(z)|^2 = |a_s(L)|^2 e^{-2\Gamma(L-z)},$$

$$|a_p(z)|^2 = |a_p(L)|^2 - \frac{k}{k_0}|a_s(L)|^2 e^{-2\Gamma(L-z)}. \tag{15}$$

Note that a_z is the normalized longitudinal electric field which is due to the space charge effect [17]:

$$a_z = \sum_l \frac{4\kappa k}{l(k+k_0)}\left[\langle\sin l\psi\rangle\cos l\psi - \langle\cos l\psi\rangle\sin l\psi\right]. \tag{16}$$

IV. RESULTS AND DISCUSSION

First, we solve the dispersion relation of Eq. (1) by the Müller method and obtain the growth rate of the scattered EM wave for three different scattering parameters ($k\lambda_D = 0, 0.2$, and 0.4). In this calculation, the beam filling factor F is assumed to be 1. Figure 1 shows the normalized growth rate (ω_i/ω_p) as a function of kv_0/Ω_{ce} for $\gamma_0 = 3$. We note that the peak occurs at $kv_0/\Omega_{ce} \simeq 9$, which reveals the resonance condition $\omega_R \simeq 4\gamma^2\omega_0$. We observe that as the energy spread increases, the growth rate curve broadens and the peak values decreases.

Figure 2 shows the normalized growth rate (ω_i/ω_p) for three different strengths of the axial guide magnetic field ($\Omega_{ce}/\omega_p = 3.0, 6.5$, and 10.0). The ratio of the electron cyclotron frequency to the pump frequency, ($r^* = \Omega_{ce}/\gamma\omega_0$), represents a measure of the approach to the resonance condition. For $\Omega_{ce}/\omega_p = 3.0, 6.5$, and 10.0, the r^* values are 0.620, 0.847, and 0.923, respectively. The growth rate shows a slight increase with increasing axial guide field, indicating group-I characteristics (the increase of the growth rate with approaching gyroresonance) [12,21].

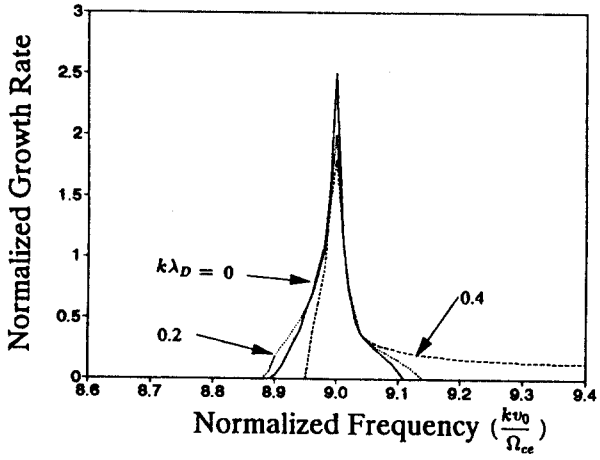

Fig. 1. Normalized growth rate (ω_i/ω_p) vs. the frequency of the scattered EM wave for three scattering parameters. The solid line indicates the $k\lambda_D = 0$ case, the dotted line indicates $k\lambda_D = 0.2$, and the dashed line indicates $k\lambda_D = 0.4$.

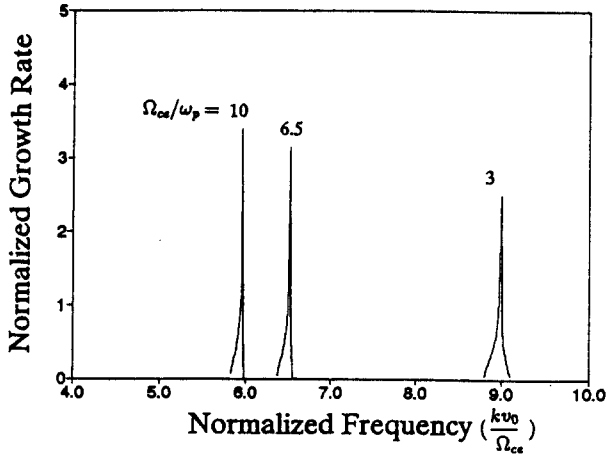

Fig. 2. Normalized growth rate (ω_i/ω_p) vs. the frequency of the scattered EM wave for three values of Ω_{ce}/ω_p (3.0, 6.5, and 10.0).

Figure 3 shows the variation of the normalized growth rate as a function of the relativistic factor of the electron beam. It is well known that the power gain (or the growth rate) is proportional to λ_0/γ^3 [12,21]. Since the pump frequency is chosen as the cutoff frequency given in Eq. (3), the variation of the growth rate with the relativistic factor results from a combination of the effects of the pump frequency and the relativistic factor. At low γ, the effect of the relativistic factor is rather small compared to that of the reduced pump frequency, so the growth rate increases with γ. At medium γ, however, the effect of the Doppler shift ($4\gamma^2$) becomes dominant over that of the reduction of the pump frequency; thus, the growth rate decreases again with increasing γ.

Using the Eqs. (7)–(12), we calculate numerically the amplified wave amplitude throughout the interaction region and the nonlinear efficiency (or power gain) of the FEL system following the self-consistent evolution of the

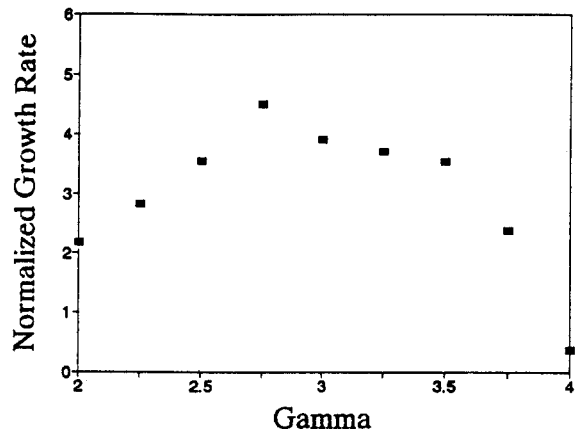

Fig. 3. Normalized growth rate (ω_i/ω_p) vs. the relativistic factor of the electron beam.

amplitude and the phase of the wave. The propagation of the wave is described by the paraxial difference method on a spatial grid on axis with 800 grid points. About 400 test particles that are loaded with uniformly distributed phases move in γ, ψ space according to Eqs. (7) and (8).

From the nonlinear particle simulation, we obtain results which exhibit similar characteristics to those of the results of linear analysis (Figs. 1–3). Since the operating regions discussed in this particle simulation pertain to group-I orbits, the results show that the gain (or the extraction efficiency) decreases with increasing γ and increases with larger axial guide magnetic field.

Figures 4 and 5 show the power along the interaction region using the particle simulation based on Eqs. (7)–(12). It should be noted that neither case has saturated. The saturation behavior will be dealt with in a subsequent paper. We consider the two pump wavelengths, 0.2 cm (gyrotron) and 10.6 μm (CO_2 laser). With an electron beam energy of $\gamma = 3$, the output wavelengths of the scattered wave for these two pump wavelengths are 55 μm and 0.3 μm, respectively.

Figure 4 is the result for the gyrotron-powered EM pump (wavelength 0.2 cm, strength 4.79×10^7 (V/m)). The electron-beam current density is 10^8 (A/m^2), and we consider three cases of energy spread ($\gamma = 3$, $(\Delta\gamma/\gamma)_{max} = 0\%, 0.5\%$, and 1%). As can be noted, the appreciable energy spread causes no exponential growth of the scattered radiation. The simulation results indicate that in parameter region of Figs. 4–5, the space charge field of Eq. (16) is negligible compared with the ponderomotive force. However, for the Raman (high current, weak pump) region, this term plays a significant role [18].

Figure 5 shows the output power when the EM pump has a wavelength of 10.6 μm (CO_2 laser) [22] and a field strength of 6×10^9 V/m. In this case, the energy spread gives rise to no power gain at all. The case of $(\Delta\gamma/\gamma)_{max} = 0.5\%$ exhibits a more severe power decrease than the $(\Delta\gamma/\gamma)_{max} = 1.0\%$ case. This may be due to a numerical error. Thus, we can note that for the high-

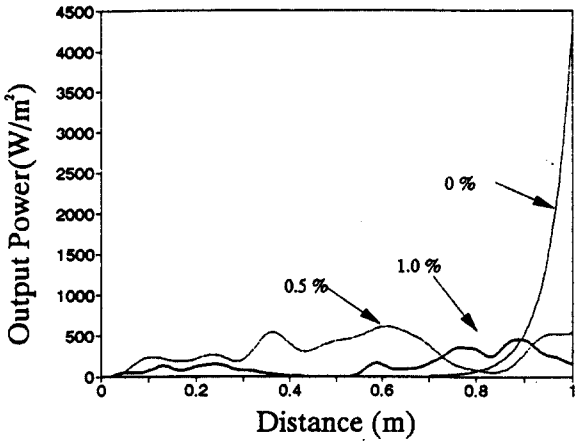

Fig. 4. Power (W/m^2) along the interaction region for three values of the energy spread ($(\Delta\gamma/\gamma)_{max}$ = 0%, 0.5%, and 1%). Here, the pump wavelength is 0.2 cm. An arbitrarily chosen input field strength of 10^2 (V/m) is used.

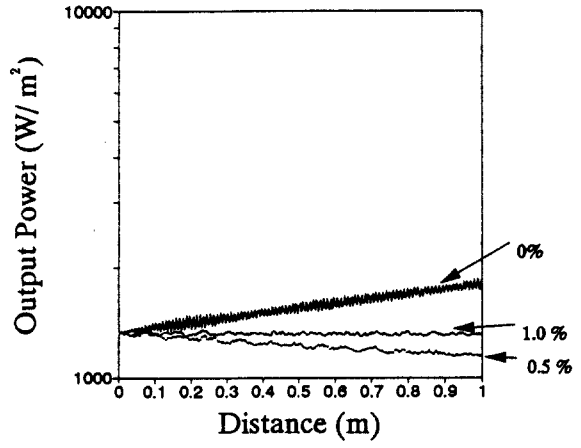

Fig. 5. Power (W/m^2) along the interaction region for the CO_2 laser pump. Three values of the energy spread are shown. An abitrarily chosen input field strength of 10^6 (V/m) is used.

frequency region, the electron-beam quality is crucial.

Since the pump wavelength of a CO_2 laser makes the K-value too small (in Fig. 5, $K = 0.02$), the quivering velocity $\beta_\perp (= K/\gamma_0)$ also becomes very small. If the laser is focused to a few mm in diameter and the intensity is higher than 10^{14} W/cm^2, then the undulator parameter K can be greater than 0.1. For instance, if the CO_2 laser intensity at the beam waist is 5×10^{14} W/cm^2, the strength of the pump electric field E_0 has a value of 6.13×10^{10} V/m. With larger value of K, we can expect large power gains.

In addition to the above, we observe the following from a series of simulation runs: (1) There exists no instability for the LHCP wave. (2) For higher pump frequency, the maximum growth rate becomes smaller and the lineshape is broader. (3) For higher energy electron beams than $\gamma = 4$, the growth rate decreases rapidly.

V. CONCLUSIONS

In this study we solve numerically the linear dispersion relation, including the beam energy spread, for an electromagnetically pumped FEL. Using the one-dimensional Maxwell-Lorentz formulation, we perform a particle simulation of the beam transport along the interaction region for various pump conditions. The model operating parameters are chosen from on-going (or planned) experiments. Modeling of the beam emittance and the space charge effects with an equivalent axial energy spread (or scattering parameter) allows consideration of only the longitudinal velocity modulation. We discuss the effect of the axial guide field, the beam energy and energy spread, and the pump strength. The main results indicate that in the millimeter-wavelength region, the axial guide magnetic field is useful for beam confinement and gain enhancement and that the electron beam quality is crucial, especially for the high-frequency region. A next step will be a parameter study which can eliminate the instabilities harmful to FEL interaction, such as the two-stream instability, the beam-breakup instability, and the Weibel instability. Also, some study to further investigate a mechanism to enhance the power gain should be undertaken [23].

ACKNOWLEDGMENTS

The authors would like to thank Professor Yoonho Seo of Kwangwoon University for useful discussions. This work was supported by the Research Division of Dong-A University and by the Korea Ministry of Education, Basic Science Research Institute Program.

REFERENCES

[1] D. A. G. Deacon, L. R. Elias, J. M. J. Madey, G. T. Ramian, H. A. Schwettman and T. I. Smith, Phys. Rev. Lett. **38**, 892 (1977).
[2] S. Watanabe *et al.*, J. Opt. Soc. Am. **B6**, 1870 (1989).
[3] Yoonho Seo and Tae Hwan Kim, J. Korean Phys. Soc. **25**, 319 (1992).
[4] T. Shintake, K. Huke, J. Tanaka, I. Sato and I. Kumabe, Jpn J. Appl. Phys., **22**, 844 (1983).
[5] B. G. Danly, G. Bekefi, R. C. Davidson, R. J. Tempkin, T. M. Tran and J. S. Wurtele, IEEE J. Quantum Electron. **QE-23**, 103 (1987).
[6] T. M. Tran, B. G. Danly and J. S. Wurtele, IEEE J. Quantum Electron. **QE-23**, 1578 (1987).
[7] T. S. Chu, B. G. Danly and R. Temkin, Nucl. Instr. and Meth. **A285**, 246 (1989).
[8] E. Esarey, P. Sprangle, A. Ting and S. K. Ride, Nucl. Instr. Meth. **A331**, 545 (1993).
[9] J. C. Gallardo, Nucl. Instr. Meth. **A341**, ABS 74, (1994).
[10] J. Kupersztych, Phys. Rev. Lett. **70**, 770 (1993).
[11] J. Gea-Banacloche, G. Moore, R. Schicher, M. Scully and

H. Walther, IEEE J. Quantum Electron. **QE-23** 1558 (1978).
[12] Tae Hun Chung, J. Korean Phys. Soc. **24**, 460 (1991).
[13] H. R. Hiddleston and S. B. Segall, IEEE J. Quantum Electron. **QE-17**, 1488 (1981).
[14] S. D. Conte and Carl de Boor, *Elementary Numerical Analysis* (Mcgraw-Hill, 1980)
[15] C. W. Roberson and P. Sprangle, Phys. Fluids B1, 3 (1989).
[16] P. Sprangle and C. M. Tang, Appl. Phys. Lett. **39**, 677 (1981).
[17] Tae Hun Chung and Jae Koo Lee, J. Phys. Soc. Jpn. **62**, 2510 (1993).
[18] Yoonho Seo, Phys. Fluids B**3**, 797 (1991).
[19] H. P. Freund and T. M. Antonsen Jr., *Principles of Free-electron Lasers* (Chapman and Hall, London, 1992), pp. 412-417.
[20] P. L. Similon and J. S. Wurtele, Phys. Fluids B1, 1307 (1989).
[21] H. P. Freund, R. A. Kehs and V. L. Granatstein, Phys. Rev. A**34**, 2007 (1986).
[22] K. Mima *et al.*, Nucl. Instr. and Meth. A**272**, 106 (1988); N. Ohigashi *et al.*, Nucl. Instr. and Meth. A**259**, 111 (1987).
[23] B. L. Qian, Y. G. Liu and C. L. Li, Phys. Plasmas **1**, 4089 (1994).